

An EHT based model for Single Molecule Incoherent Resonant Scanning Tunneling Spectroscopy

Hassan Raza

NSF Network for Computational Nanotechnology and School of Electrical and Computer Engineering,
Purdue University, West Lafayette, Indiana 47907 USA.

We report Extended Hückel theory (EHT) based mean-field incoherent Non-equilibrium Green's function (NEGF) transport model, for single molecule scanning tunneling spectroscopy (STS), with dephasing due to elastic and inelastic scattering within the self-consistent Born approximation (SCBA) and report a procedure for tip modeling based on EHT basis set modification. We use this model to study the effect of the temperature dependent elastic dephasing, due to low energy phonon modes in far-infrared range for which $\hbar\omega \ll k_B T$, on the *resonant* conduction through highest occupied molecular orbital (HOMO) level. Furthermore, we report inelastic *off-resonant* tunneling results, showing peak in second derivative due to one phonon mode. Finally, we suggest that dephasing should be included in room temperature molecular transport calculations.

PACS numbers: 72.10.-d, 81.07.Nb, 85.65.+h

I. INTRODUCTION

This paper is focused on presenting an Extended Hückel theory (EHT) based self-consistent mean-field transport model for incoherent single molecule spectroscopy. Although simple, this approach is worth pursuing because EHT overcomes many of the shortcomings of the more sophisticated theories, *e.g.* density functional theory (DFT), etc. Furthermore, the simplicity and the exponential dependence of the basis set in EHT allows a very intuitive solution to tip modeling as described in this paper. The proper tip modeling is very important because if condensed matter like orbitals are used for calculating transport properties, to get experimentally observed current values, one has to bring the tip very close to the molecule [about 4-5 Å]. This results in wrong voltage drop [higher than the actual] across the molecule and hence, an error is introduced in the calculation.

Apart from this, electron-phonon scattering in molecular structures on different metallic substrates has been studied quite extensively at low temperature both experimentally [1, 2, 3, 4] and theoretically [5, 6, 7, 8, 9] in the form of off-resonant inelastic tunneling spectroscopy (IETS). In IETS, different phonon modes give distinct peaks in the second derivative of current-voltage (I-V) characteristics. Therefore, it is no surprise that IETS has been used as a probe for molecular conduction. Here, we refer to phonons as the quantized vibrational modes, also called vibrons, of a molecule. Thus, in our analysis, the molecule acts as the scattering region similar to Refs. [5, 6, 7, 8]. Physically, electron-phonon scattering leads to inelastic dephasing. As a result, not only the phase of an electron is irreversibly lost due to phonon degree of freedom but is also exchanges energy with the phonon bath in discrete quanta of energy $\hbar\omega$. Therefore, an electron at energy E can absorb a phonon of energy $\hbar\omega$ to acquire $E + \hbar\omega$ energy following energy conservation principle. Similarly, it can emit a phonon of energy

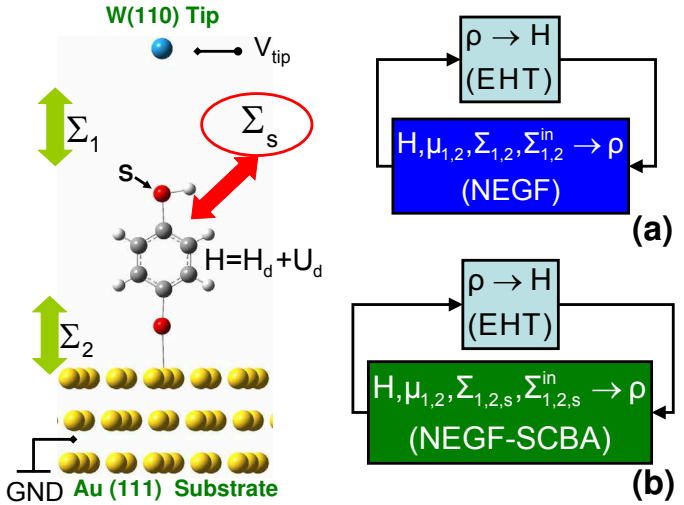


FIG. 1: (color online) Schematic diagram. Scanning Tunneling Spectroscopy (STS) setup for probing conduction through phenyl/benzene dithiol (PDT/BDT) molecule bonded to Au(111) substrate. Voltage is applied at the tungsten W(110) tip. (a) A schematic showing the self-consistent procedure of solving EHT-NEGF equations for coherent transport [20]. (b) A schematic detailing the self-consistent procedure of solving EHT-NEGF-SCBA equations for quantum transport with elastic and inelastic dephasing.

$\hbar\omega$ to end up at $E - \hbar\omega$ energy. If $\hbar\omega$ of a phonon mode is less than a characteristic energy (*e.g.* $k_B T$), this inelastic dephasing process can be approximated by an elastic one for mathematical and numerical convenience without affecting the physical results. However, conceptually there is a big difference between elastic and inelastic dephasing. In the former, all the energy channels are independent, whereas in the latter energy channels are coupled. This means that the electron density at a particular energy E depends on the electron and hole densities at different energies $E \pm \hbar\omega$ for the inelastic dephasing in contrast

to the electron density at energy E only depending upon the electron and hole densities at the same energy E for the elastic dephasing.

It should be noted that the phonon modes of a molecule bonded to a substrate can be very different from those of the same molecule in gas phase. As an example, the organic molecules in gas phase have characteristic vibrational frequencies in the infrared range, *i.e.* $1000 - 3000\text{cm}^{-1}$, which is roughly equal to $80-250\text{meV}$. However, experimental data, obtained using IETS [3] and high energy electron energy loss spectroscopy (HREELS) [10], is suggestive that these molecules, when bonded to a substrate, *e.g.* $\text{Au}(111)$, lead to very low energy phonon modes in the far-infrared range, *i.e.* Theoretically [6, 7], dominant modes less than about 10meV have been clearly reported. Since the experimental results are suggestive, further experiments need to be done to put this issue on a solid footing. These far-infrared modes are the result of the combined motion of the molecule with respect to the substrate. Furthermore, most of these infrared modes are longitudinal modes and couple very well with electrons. Hence, the low energy phonon modes, for which $\hbar\omega \ll k_B T$ at room temperature, are the most important phonon modes for molecules bonded to substrates as compared to high energy modes in gas phase. Apart from this, to the best of our knowledge, the effect of electron-phonon scattering on the resonant molecular transport at room temperature has not yet been studied in detail. In a previous study [11], we report transport calculations at room temperature for a styrene chain bonded to $n^{++}\text{-H:Si}(001)$ substrate where experimentally observed I-V characteristics cannot be reproduced without including elastic dephasing due to these low energy electron-phonon scattering events.

In this paper, we theoretically study incoherent scanning tunneling spectroscopy (STS) of a phenyl/benzene dithiol (PDT/BDT) molecule, bonded to $\text{Au}(111)$ substrate, using a tungsten $\text{W}(110)$ tip as shown in Fig. 1. In context of molecular spectroscopy and conduction, there are three sources of broadening, (1) contact broadening which is temperature independent (2) the Fermi function broadening of the two contacts, which is temperature dependent and (3) broadening due to electron-phonon scattering which is also temperature dependent. The main focus of this work is the broadening due to this third source. In this context, we focus on the electron-phonon scattering due to low energy phonons, which are the most important modes for molecules bonded to substrates.

The paper is divided into six sections. In Sec. II, we provide the mean-field self-consistent EHT-NEGF-SCBA model for studying transport with dephasing due to electron-phonon scattering. In Sec. III, details are provided with the electrostatic calculation. Tip modeling is a very important aspect of the calculations and is discussed thoroughly in Sec. IV. In Sec V, we discuss the results and report the temperature dependence of the transport quantities on the electron-phonon scattering due to low energy phonons. Furthermore, we report

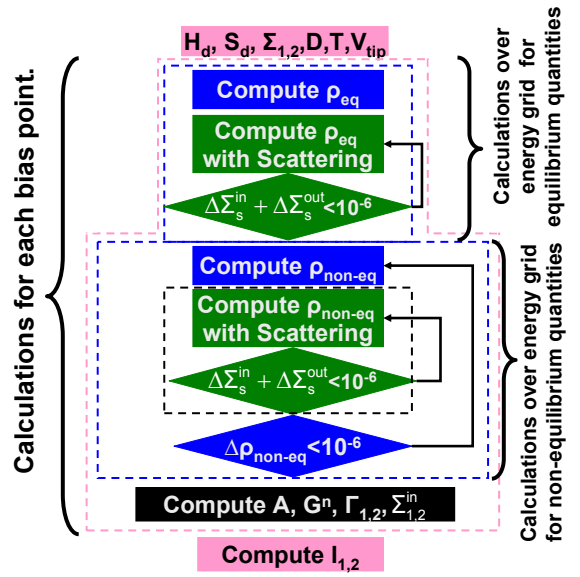


FIG. 2: (color online) Block diagram for transport with elastic dephasing. For elastic dephasing, all the energy channels are independent. Therefore, energy dependent quantities can be calculated independently for each energy point with the convergence criteria shown. Thus, equilibrium and non-equilibrium quantities for each bias point are calculated as shown. The green and blue blocks are color coded to match with the blocks in Fig. 1(a,b). For inelastic dephasing, since energy channels are coupled, one has to use convergence criteria on the calculated energy dependent quantities over the whole energy range.

the calculated IETS spectrum to show the effectiveness of the method. Finally in Sec. VI, we provide the conclusions. All the molecular visualization is done using GaussView [12]. Furthermore, we do not account for the possible structural changes due to temperature variation and/or applied tip voltage in this work.

II. FORMALISM

We use the single particle non-equilibrium Green's function formalism (NEGF) in the mean field approximation using non-orthogonal basis to model the quantum transport. We define the retarded non-equilibrium Green's function in non-orthogonal basis as:

$$G(E, V_{tip}) = [(E + i0^+)S - H - E_{fc}S - \Sigma_{1,2} - \Sigma_s]^{-1} \quad (1)$$

where S is the overlap matrix and $H = H_d + U_d$. H_d is the device Hamiltonian for an isolated molecule expressed in Extended Hückel theory (EHT) [13]. Since, there is no vacuum reference in EHT parametrization, we use input from experiments or other sophisticated theoretical methods to set the reference. E_{fc} , thus, is used as an adjusting parameter to achieve this objective. In this paper, it is assumed to be 2eV unless otherwise specified. Furthermore, the electronic structure of

Au(111) and W(110) tip is also calculated within EHT, which is further used in calculating self-energies ($\Sigma_{1,2}$) due to the tungsten W(110) tip and Au(111) contacts respectively. In this paper, we do not go into the details about EHT which is a standard quantum chemistry technique. The conventions for the symbols used are same as those of Refs. [14, 15] and the symbols used elsewhere are put in brackets for completeness and clarity. U_d incorporates both Laplace's potential due to the applied tip voltage (V_{tip}) and Poisson's (Hartree part only) potential due to the non-equilibrium density of electrons in the molecular channel. Electrostatics is further discussed in Sec. III. The contact self-energies $\Sigma_{1,2}$ are related to the broadening functions as $\Gamma_{1,2} = i(\Sigma_{1,2} - \Sigma_{1,2}^\dagger)$. Σ_1 is the tip self-energy, which is further discussed in Sec. IV. Σ_2 , the Au(111) self-energy is discussed in Ref. [20]. Σ_s , the scattering self-energy, is discussed later in this Sec. The spectral function is defined as $A = i(G - G^\dagger)$, which is related to the density of states of the molecular region as $D(E) = 2(for\ spin)tr(AS)/2\pi$. The electron correlation function $G^n (= -iG^<)$ is given as:

$$G^n = G(\Sigma_1^{in} + \Sigma_2^{in} + \Sigma_s^{in})G^\dagger \quad (2)$$

where $\Sigma_{1,2}^{in} (= -i\Sigma_{1,2}^<)$ are the contact inflow functions defined as $\Gamma_{1,2}f_{1,2}$ and $\Sigma_s^{in} (= -i\Sigma_s^<)$ is the scattering inflow function, to be further discussed below. $f_{1,2}(E)$ are the contact Fermi functions defined as $1/[1 - \exp((E - \mu_{1,2})/k_B T)]$. $\mu_{1,2}$ are the chemical potentials of the two contacts given as $\mu_1 = \mu_o - qV_{tip}$, $\mu_2 = \mu_o$ respectively and μ_o is the equilibrium chemical potential. In this formalism, contacts are assumed to remain in equilibrium

with the applied voltage due to dissipative processes inside the contacts. This is a valid assumption for metallic and degenerately doped semi-conducting contacts. However for the moderately doped or lightly doped semi-conducting contacts, there would be band bending due to V_{tip} and these contacts may go out of equilibrium. This band bending should be included in transport calculations, thus making it a very challenging computational problem to work on. Moreover, the hole correlation function is defined as $G^p = A - G^n$. The electron density matrix is given as:

$$\rho = \frac{1}{2\pi} \int_{-\infty}^{\infty} dE G^n(E) \quad (3)$$

using the above expression for electron density, the total number of electrons is computed as $N = 2(for\ spin)tr(\rho S)$. Finally, the current voltage (I-V) characteristics are computed as follows [14, 15, 16]:

$$I_i(V_{tip}) = 2(for\ spin) \frac{e}{h} \int_{-\infty}^{\infty} dE tr(\Sigma_i^{in} A - \Gamma_i G^n) \quad (4)$$

Since Σ_s , G , G^n and Σ_s^{in} depend on each other, we solve for the above four quantities self-consistently along with the main self-consistent loop of applied voltage as shown in Fig. 1(a,b). The flow diagram for the self-consistent procedure at each bias is shown in Fig. 2. For such a solution, it can be shown that $I_s(V_{tip})$, which is the current through the 'scattering contact', is always zero.

The scattering inflow function, outflow function and broadening function are defined as [17]:

$$\Sigma_s^{in}(E) = \int_0^{\infty} \frac{d(\hbar\omega)}{2\pi} D^{em}(\hbar\omega) SG^n(E + \hbar\omega) S + D^{ab}(\hbar\omega) SG^n(E - \hbar\omega) S \quad (5)$$

$$\Sigma_s^{out}(E) = \int_0^{\infty} \frac{d(\hbar\omega)}{2\pi} D^{em}(\hbar\omega) SG^p(E - \hbar\omega) S + D^{ab}(\hbar\omega) SG^p(E + \hbar\omega) S \quad (6)$$

$$\Gamma_s(E) = \Sigma_s^{in} + \Sigma_s^{out} = \int_0^{\infty} \frac{d(\hbar\omega)}{2\pi} D^{em}(\hbar\omega) S [G^n(E + \hbar\omega) + G^p(E - \hbar\omega)] S + D^{ab}(\hbar\omega) S [G^n(E - \hbar\omega) + G^p(E + \hbar\omega)] S \quad (7)$$

where $D^{em}(\hbar\omega) = (N + 1)D_o(\hbar\omega)$ and $D^{ab}(\hbar\omega) = N D_o(\hbar\omega)$ are emission and absorption dephasing functions respectively. N is the equilibrium number of phonons given by Bose-Einstein statistics as $1/[\exp(\hbar\omega/k_B T) - 1]$. It is straight forward to show that for a particular phonon mode, $D^{ab}/D^{em} = \exp(-\hbar\omega/k_B T)$. Eq. 5 physically implies that electron inflow at a particular energy E is dependent on the electron correlation function G^n (which physically gives energy resolved electron density) at energy $E + \hbar\omega$ for

phonon emission and $E - \hbar\omega$ for phonon absorption. One would expect the trend to be reversed for the electron outflow as shown in Eq. 6. The overall broadening due to this scattering process is given by $\Gamma_s(E)$, which is the sum of the inflow function and outflow function. For a particular phonon mode $\hbar\omega$, $D_o(\hbar\omega)$ is a fourth ranked tensor and is related to the electron phonon interaction potential as $\langle i, j | U^\dagger U | k, l \rangle$, where U is the electron-phonon interaction potential. Physically it states that an electron in state $|k, l \rangle$ can be scattered into the

state $|i, j\rangle$ due to this inelastic electron-phonon scattering event. Thus, not only $D_o(\hbar\omega)$ is different for different phonon modes, but can be different for different molecular orbitals as well and can be explicitly written as $D_o(i, j; k, l; \hbar\omega)$. One point to note is that Eqs. 5-7 are modified from those reported in Ref. [17] for non-orthogonal basis as discussed by F. Zahid *et al* [18].

High energy phonon limit: For $\hbar\omega \gg k_B T$, we have $N \approx 0$ and $N+1 \approx 1$, hence $D^{em} \approx D_o$ and $D^{ab} \approx 0$. In such a case, Eq. 7 becomes:

$$\Gamma_s(E) = \int_0^\infty \frac{d(\hbar\omega)}{2\pi} D_o(\hbar\omega) S[G^n(E + \hbar\omega) + G^p(E - \hbar\omega)]S \quad (8)$$

Thus at low temperature, e.g. at 4K where $k_B T \approx 0.3\text{meV}$, phonon modes having energy greater than 0.3meV (e.g. 5meV or more) contribute to IETS spectrum through the emission of phonons. The contribution due to absorption is negligible in this case because enough phonons are not available to be absorbed. Moreover, as shown in Eq. 8, $\Gamma_s(E)$ is temperature independent. Thus, the broadening due to electron-phonon scattering in this case is temperature independent, apart from the Fermi function dependence of $G^{n,p}$. Hence, the only temperature dependent broadening is the Fermi broadening. Apart from this, the contribution of a phonon mode at low temperature for which $\hbar\omega \gg k_B T$ implies that at room temperature if $k_B T$ becomes much higher than $\hbar\omega$, it would lead to much stronger dephasing. This is further discussed below.

Low energy phonon limit: For low energy phonons where $\hbar\omega \ll k_B T$, it can be shown that $N+1 \approx N \approx k_B T/\hbar\omega$, which leads to,

$$\Gamma_s(E) = \int_0^\infty \frac{d(\hbar\omega)}{2\pi} [D^{em}(\hbar\omega) + D^{ab}(\hbar\omega)] S A(E) S \quad (9)$$

and

$$D^{em}(\hbar\omega) \approx D^{ab}(\hbar\omega) = N D_o(\hbar\omega) \approx \frac{k_B T}{\hbar\omega} D_o(\hbar\omega) \quad (10)$$

We finally obtain $\Gamma_s(E)$ as,

$$\Gamma_s(E) \approx T \underbrace{\int_0^\infty \frac{d(\hbar\omega)}{2\pi} \frac{2k_B D_o(\hbar\omega)}{\hbar\omega}}_D S A(E) S \quad (11)$$

where D is referred to as Dephasing strength for the low energy phonon limit in this paper. Eq. 11 physically states that scattering broadening function is directly proportional to temperature. Since broadening due to dephasing is dependent on $\Gamma_s(E)$, it is worthwhile to appreciate the temperature dependence of this quantity. One can visualize that at 4K, if phonon modes less than 25meV ($k_B T$ at 300K) but more than 0.3meV ($k_B T$ at 4K) give very strong IETS spectrum, it means that D_o corresponding to these modes is appreciable. With increasing temperature, the dephasing strength (D) due to

these modes increasing rapidly due to exponential dependence of Bose-Einstein factor on temperature. In fact, in the temperature range where $\hbar\omega \ll k_B T$, this dephasing strength would be proportional to the temperature and inversely proportional to $\hbar\omega$ as shown in Eq. 11, thus making the low energy phonon modes much more important at room temperature as compared to being important at low temperature.

Furthermore, by definition the real part of $\Sigma_s(E)$ is computed by taking a Hilbert transform of the imaginary part as below,

$$\Sigma_s(E) = \frac{1}{\pi} \int_{-\infty}^\infty dy \frac{-\Gamma_s(y)/2}{E - y} - i\Gamma_s(E)/2 \quad (12)$$

Calculating the real part of $\Sigma_s(E)$ is computationally very expensive and leads to convergence issues. Previously, it has been reported, based on extensive calculations [8], that this real part contributes on the order of meV. Therefore, we ignore it in this paper. Apart from this, we do not calculate the phonon modes and the corresponding dephasing strength D, which is a fourth ranked tensor, but we phenomenologically approximate it by a constant. This approximation seems to be reasonable as reported in a previous work [11].

With reference to the previous theoretical work, this paper is unique in the sense that a computationally inexpensive self-consistent EHT based theoretical framework is presented for incoherent STS with full 3D electrostatics including image potentials. Notably, T. Frederiksen *et al* [5], N. Sergueev *et al* [6], Y.-C. Chen *et al* [7], M. Paulsson *et al* [8] and T. Rakshit *et al* [19] have reported DFT based approaches for inelastic dephasing. F. Zahid *et al* [18] have used EHT based Büttiker probe technique [which includes elastic dephasing] for numerical convenience. Our work is unique in the sense that (1) we incorporate proper tip modeling (2) we include full 3D electrostatics with Image charge correction and Hartree potential under non-equilibrium conditions and (3) we apply the model to study resonant tunneling regime, whereas previously these models have been applied to only off-resonant tunneling to study IETS. However we do not calculate D, same as F. Zahid *et al* [18] and T. Rakshit *et al* [19], in contrast with Refs. [5, 6, 7, 8], where proper D is calculated.

III. ELECTROSTATICS

For solving electrostatics, we follow the approach used in Ref. [20] and briefly describe the procedure here. Interested readers can consult Ref. [20] for a detailed description. 3D Laplace's equation is solved using the finite-element (FE) method to obtain the potential profile across styrene due to V_{tip} . This method also provides the zero bias band line up potential due to the Fermi level mismatch of 0.1eV between Au(111) and W(110) tip, whose work functions are 5.1eV and 5.2eV respectively. The Poisson potential for the molecule is approximated

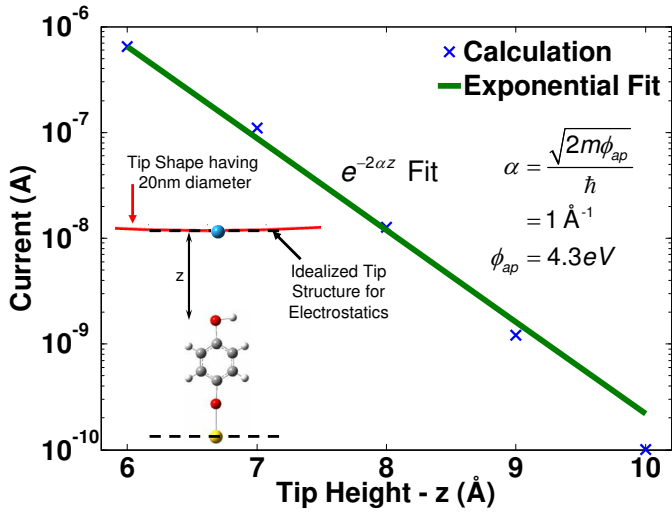


FIG. 3: (color online) Tip modeling. The calculated current (I) for $V_{tip} = 1V$ as a function of tip-molecule distance (z) showing exponential dependence of current on z . The extracted barrier height from this I - z plot is 4.3eV , whereas with original parameters it is approximately 10eV . The calculated apparent barrier height (ϕ_{ap}) is close to the work functions of the contacts being used. Furthermore, for calculating Laplace and Image potential due to V_{tip} , tip is approximated by a flat metallic surface. The inset shows a visual justification for this approximation where the black dotted line represents the flat surface and red solid line is the actual tip shape with 20nm diameter. The tip is 7\AA away from the molecule in this case.

via the complete neglect of differential overlap method [21]. Image effects are incorporated to ensure that self-consistency is not over-estimated, which can alter the results significantly. In all of the above electrostatic calculations, the tip is assumed to be a metal sheet having work function of 5.2eV . Furthermore, we include the voltage self-consistency for elastic dephasing only. Since, we are studying the inelastic dephasing in the off-resonance regime, self-consistency is not important.

IV. TIP MODELING

Since the last tip atom dominates STS, we use a single tungsten (W) atom as tip. This assumption is for a "good" tip that can be used for atomic resolution microscopy and spectroscopy, where there are no adsorbate or multiple tip structures. A typical tip has a diameter on the order of 20nm or more. However, the exact tip shape and structure remains to be unknown. We use W(110) configuration, because structurally it is the lowest energy state. However, the only property we use for this configuration is the work function, which is 5.2eV , for calculating the zero bias band line up potential, which shifts the molecular levels. For 5.2eV work function, the Fermi level mismatch is 0.1eV and the shift in molecular levels due to this mismatch is approximately 0.015eV , if

tip is 10\AA away from the molecule. Thus, taking any different tip configuration having different work function would cause a shift of few meV in the spectroscopic features.

Electrostatically, for a tip having approximately 20nm diameter, the tip looks relatively flat as shown in the inset of Fig. 3. In other words, the electrostatic voltage drop across the molecule is insensitive to considering actual shape (which is unknown) and flat surface if the tip is really close to the molecule. One can visually inspect the difference to appreciate this assumption for a tip atom 7\AA away from the molecule as shown in the inset of Fig. 3. At the tip atom (the blue one), the black dotted line is the flat surface that we use in our calculations. The shifted red solid line is the portion of a tip having 20nm diameter. It can be seen that the difference between the two is very small.

On the other hand, at such a small tip-molecule distance, electronic effects due to wave-function overlap between the tip and the molecule become significantly important. In this perspective, proper modeling of decay of current (I) with varying tip-molecule distance (z) becomes impeding. Apparent barrier height (ϕ_{ap}) is then calculated from the slope of the $\log(I)$ - z plot as discussed in Ref. [22]. As an example, with unmodified parameters, we obtain a barrier height of approximately 10eV . We report a scheme for modifying basis set of tip atom to get correct apparent barrier height. This has been done before in the context of scanning tunneling microscopy [23]. We modify the EHT parameters of the s-orbital basis set [24] for tungsten atom and obtain $\phi_{ap} = 4.3\text{eV}$ from the calculated I - z plot with $V_{tip} = 1V$ as shown in Fig. 3. This I - z plot is for coherent transport without any voltage self-consistency.

The above parameter modification affects S_1 and H_1 , provided the tip self-energy Σ_1 is defined as $[(E + i0^+)S_1 - H_1]g_{s1}((E + i0^+)S_1^\dagger - H_1^\dagger)$, where g_{s1} is the surface Green's function for the tip. We assume a constant g_{s1} , calculated from the density of states at equilibrium chemical potential of bulk tungsten $D_W(\mu_o)$, i.e. $g_{s1} = -i\pi D_W(\mu_o)$. However, Σ_1 is still energy dependent and this energy dependence should in fact capture all the barrier tunneling effects. The only experimental features it would not be able to capture are the ones due to peculiar electronic structure of tip as in Ref. [25].

Previously in theoretical STS calculations, atomic like orbitals have been used for tip modeling resulting in artificially broadened spectroscopic features in comparison with the experiments. However, these calculations result in higher current levels than experiments. Not only this, the apparent barrier height was larger than the work function of the materials being used, which is unphysical. In this paper, we have tried to address and solve these problems.

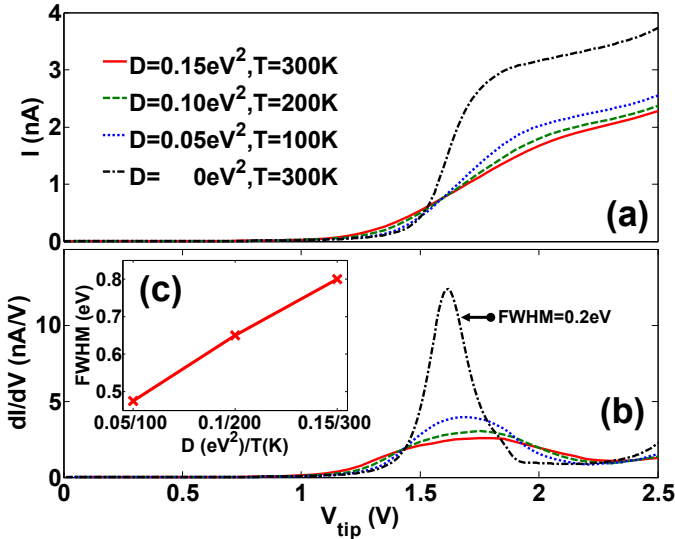


FIG. 4: (color online) Effect of temperature on the incoherent resonant conduction through the highest occupied molecular orbital (HOMO) level with elastic dephasing due to low energy electron-phonon scattering. The dephasing strength (D) is directly proportional to the temperature (T). Thus, the additional broadening due to elastic dephasing decreases with decreasing temperature in a linear fashion. (a) I-V characteristics showing broadening of spectroscopic features due to dephasing. (b) dI/dV - V characteristics providing an alternate and more detailed view of broadening of spectroscopic features [legend same as that of part (a)]. (c) Full width half maximum (FWHM) of the first conductance peak corresponding to the HOMO level showing linear dependence on temperature. The dephasing strength (D) is assumed to be 1.5eV^2 at 300K. D at any other temperature T is computed as $D(T) = \frac{D(300\text{K})}{300\text{K}} \times T(\text{in K})$.

V. RESULTS

In this section, we apply the reported EHT-NEGFF-SCBA model to incoherent transport (with elastic dephasing) through the highest occupied molecular orbital (HOMO) level of a PDT/BDT molecule bonded to a Au(111) substrate through a single Au-S bond and probed using a tungsten W(110) tip as shown in Fig. 1. Au-S bond length is the standard 2.53Å and tip molecule distance is taken to be 10Å. The dephasing strength (D) at 300K is assumed to be 0.15eV^2 . Dephasing strength at any other temperature T is then calculated as $D(T) = \frac{D(300\text{K})}{300\text{K}} \times T(\text{in K})$ following Eq. 11.

The calculated current-voltage (I-V) characteristics are shown in Fig. 4(a). For $D=0$, *i.e.* for coherent conduction through PDT/BDT molecule at 300K, the I-V curve has a sharp rise. Fig. 4(b) provides an alternate view of part (a) showing the corresponding conductance-voltage (dI/dV - V) characteristics. For the coherent transport, the full width half maximum (FWHM) of the conductance peak is approximately 0.2eV. We define FWHM as the difference between the tip voltages, on either side of

the peak in the conductance curve, at which the conductance reaches half of its maximum value. This broadening is only due to (1) the finite life-time of electrons in the molecule as a result of the coupling with the contacts given by the broadening functions $\Gamma_{1,2}$ and (2) the temperature dependent broadening in the contact Fermi functions.

With $D = 0.15\text{eV}^2$ at 300K, the I-V curve gets smeared out [see Fig. 4(a)] due to an additional broadening as a result of the elastic dephasing. Not only this, the overall current level also decreases. However, it should be noticed that the current starts increasing slightly earlier and hence is slightly higher than $D=0$ case for $V_{tip} < 1.45\text{V}$. Correspondingly, the conductance (dI/dV) plot [see Fig. 4(b)] for $D = 0.15\text{eV}^2$ at 300K shows a higher conductance value for $1.45\text{V} > V_{tip} > 1.8\text{V}$, (*i.e.* before and after the conductance peak). This effect is precisely due to the additional broadening caused by the elastic dephasing. However, the peculiar features are non-trivial and we address next.

The FWHM of this conductance peak is approximately 0.8eV as shown in Fig. 4(c). The comparison of I-V and dI/dV - V plots for $D=0$ and $D = 0.15\text{eV}^2$ at 300K raises two important questions (1) why the overall current value decreases in this case due to broadening and (2) how does the temperature dependence of dephasing strength affect the FWHM of conductance peaks.

Whether the dephasing increases or decreases the current level is an important question. The answer to which depends on the energy dependence of the contact broadening functions $\Gamma_{1,2}$. But, independent of this energy dependence, the physical effect of dephasing remains the same, *i.e.* broadening of the molecular spectral function. As a result of this broadening, for a normalized spectral function, the spectral weight increases in the energy range where it was lower before and *vice versa*. If the energy region, where the spectral weight is transferred, has larger broadening functions $\Gamma_{1,2}$, as compared to the energy range where the spectral function was localized, it would result in higher current values. Similarly, if the $\Gamma_{1,2}$ is smaller in the energy range where the spectral weight is transferred, the current would decrease. We analyze the energy dependence of $\Gamma_{1,2}$ in the energy range of conduction and find that both Γ_1 and Γ_2 decrease as a function of decreasing energy, which corresponds to positive V_{tip} . This is the reason that the broadened molecular spectral function gives rise to higher current values for lower V_{tip} , where the broadening functions $\Gamma_{1,2}$ are larger. Similarly, current values are smaller for larger V_{tip} , where $\Gamma_{1,2}$ are smaller. Hence, this study with Au(111) and tungsten W(11) tip is a case where the overall current level decreases with dephasing. However, in a previous study with Si(001) we conclude that the overall current level increases with dephasing [11]. In this work, the HOMO level to start-with is near valence band-edge, where $\Gamma_2(E)$ is very small because of band edge. Without dephasing, the current is small. After including dephasing, the HOMO level gets broadened and

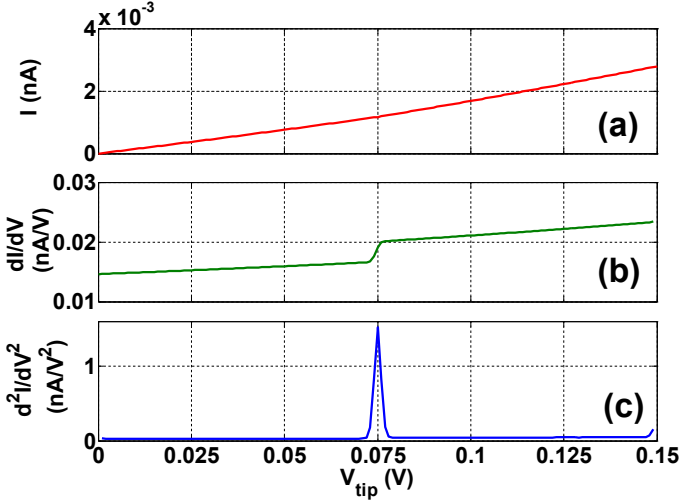


FIG. 5: (color online) Effect of inelastic scattering on the off-resonant conduction at 4K assuming one phonon mode with $D^{em} = 0.1eV^2$ and $\hbar\omega = 75meV$. (a) IETS signature is not noticeable in the I-V characteristics. (b) Inelastic scattering results in a step in dI/dV -V characteristics. (c) IETS spectra (d^2I/dV^2 -V characteristics) showing a peak at 75meV corresponding to the phonon mode. Since $\hbar\omega \gg k_BT$, $D^{ab} = D^{em}e^{-\hbar\omega/k_BT} \approx 0$. Thus, the IETS peak is due to emission of phonons and processes due to absorption of phonons are very weak.

a portion of it is in energy range where $\Gamma_2(E)$ is large. Thus, dephasing in this case results in an order of magnitude higher current.

With decreasing temperature and hence dephasing strength, namely at 200K and 100K with $D = 0.1eV^2$ and $D = 0.05eV^2$ respectively, the I-V plots [see Fig. 4(a)] follow same trends. The overall current level is larger than that at 300K with $D = 0.15eV^2$ because the molecular spectral function is concentrated in the energy range where the contact broadening functions $\Gamma_{1,2}$ are relatively higher. Similarly, the broadening in the conductance peaks is smaller than the one with $D = 0.15eV^2$ and it monotonically decreases with decreasing value of D and temperature. Furthermore, the maximum conductance value decreases with the increasing dephasing as expected. We present the calculated FWHM values of these conductance peaks to quantify the effect of dephasing as shown in Fig. 4(c). FWHM is directly proportional to the temperature and hence to dephasing strength. As discussed in Sec. II in the limit of low energy phonons, for which $\hbar\omega \ll k_BT$, scattering broadening function is directly proportional to temperature as shown in Eq. 11. The temperature dependent contribution of Fermi function is small for large tip voltages. Therefore, we conclude that the direct proportionality of FWHM of conductance peak to temperature and hence dephasing strength is due to this electron-phonon scattering. In our case, tip is far from the molecule and hence there is very small voltage drop across the molecule. Thus, the molecule is in

equilibrium with the Au(111) contact, which leads to $\Gamma_1 \ll \Gamma_2$. The dependence of FWHM of conductance peak on temperature and dephasing strength could become complicated if the tip is replaced by a good contact. However, with increasing temperature and dephasing strength, the FWHM should be asymptotically increasing. Some strange features might be expected as a result of the peculiar energy dependence of the contact broadening functions $\Gamma_{1,2}$. However, if there are temperature dependent structural changes present, the situation may get more complicated.

In Fig. 5, we report the inelastic tunneling spectroscopy (IETS) of PDT/BDT molecule at 4K. The purpose of these results is to convey the message that the model is able to handle calculations for inelastic dephasing too. We assume a single phonon mode with energy $\hbar\omega = 75meV$ and emission dephasing function $D^{em} = 0.1eV^2$. Then, the absorption dephasing function is given as $D^{ab} = D^{em}e^{-\hbar\omega/k_BT}$. Since $\hbar\omega \gg k_BT$, $D^{ab} \approx 0$, the IETS spectrum has a contribution only due to phonon emission. Fig. 5(a) shows the I-V characteristics with no feature of IETS signal. Fig. 5(b) shows the dI/dV -V characteristics with a step in the conductance curve due to emission of phonons at $eV_{tip} = \hbar\omega = 75meV$. The same signal appears as a peak in the d^2I/dV^2 spectrum as shown in Fig. 5(c).

VI. CONCLUSIONS

We have reported EHT-NEGF-SCBA model and have used it to study elastic and inelastic dephasing. It has been previously reported that low energy phonons are important in molecular conduction at low temperature [3, 6, 7, 10]. We suggest that if they are important at low temperature, they should be equally important at higher temperatures as well and should be included in calculating transport properties. Furthermore, if the energy of these modes is much less than some energy scale, *e.g.* k_BT , the effect of inelastic dephasing on transport due to such modes can be calculated using elastic dephasing. We show that within this approximation, it can be concluded that the broadening due to these low energy electron-phonon scattering is directly proportional to temperature. Whereas, in the limit of $\hbar\omega \gg k_BT$, apart from the temperature dependent broadening of Fermi function, the broadening due to electron-phonon scattering process is temperature independent. Moreover, the overall current level tends to reduce due to this dephasing. This could provide a possible solution for the observed discrepancy between theory and experiment for resonant conduction, where theoretically calculated currents are higher as compared to the experimental observations [26]. Although other mechanisms have also been suggested, *e.g.* different contact-molecule bonding [27], Coulomb blockade [28], etc. Finally, we present results for IETS to show that within the formalism, inelastic dephasing can be handled as well.

We acknowledge fruitful discussions with S. Datta. We acknowledge F. Zahid and T. Raza for Hückel-IV 3.0 [20] codes. This work was supported by the NASA Institute

for Nanoelectronics and Computing. Computational facilities were provided by the NSF Network for Computational Nanotechnology.

[1] B. C. Stipe, M. A. Rezaei and W. Ho, *Science* **280**, 1732 (1998).

[2] W. Wang, T. Lee, I. Kretzschmar and M. A. Reed, *Nano. Lett.* **4**, 643 (2004).

[3] J. G. Kushmerick, J. Lazorcik, C. H. Patterson, R. Shashidhar, D. S. Seferos and G. C. Bazan, *Nano. Lett.* **4**, 639 (2004).

[4] W. Wang and C. A. Richter, *App. Phys. Lett.* **89**, 153105 (2006).

[5] T. Frederiksen, M. Brandbyge, N. Lorente and A-P Jauho, *Phys. Rev. Lett.* **93**, 256601 (2004).

[6] N. Sergueev, D. Roubtsov and H. Guo, *Phys. Rev. Lett.* **95**, 146803 (2005).

[7] Y.-C. Chen, M. Zwolak and M. D. Ventra, *Nano. Lett.* **5**, 621 (2005).

[8] M. Paulsson, T. Frederiksen and M. Brandbyge, *Nano. Lett.* **6**, 258 (2006).

[9] A. Troisi and M. A. Ratner, *Phys. Rev. B* **72**, 033408 (2005).

[10] H. S. Kato, J. Noh, M. Hara and M. Kawai, *J. Phys. Chem. B* **106**, 9655 (2002).

[11] H. Raza, K. H. Bevan and D. Kienle, *cond-mat/0607226*.

[12] R. Dennington II, T. Keith, J. Millam, K. Eppinnett, W. L. Hovell and R. Gilliland, *GaussView, Version 3.0* (Semichem, Inc., Shawnee Mission, KS, 2003).

[13] J. Howell, A. Rossi, D. Wallace, K. Haraki and R. Hoffman, *FORTICON8*, QCPE Program 545, Department of Chemistry, Cornell University, Ithaca, NY 14853.

[14] S. Datta, *Nanotechnology* **15**, S-433 (2004).

[15] S. Datta, "Quantum Transport: Atom to Transistor", Cambridge University Press (2005).

[16] Y. Meir and N. S. Wingreen, *Phys. Rev. Lett.* **68**, 2512 (1992).

[17] G. D. Mahan, *Phys. Rep.* **145**, 251 (1987).

[18] F. Zahid, M. Paulsson and S. Datta, "Electrical Conduction through Molecules", in *Advanced Semiconductors and Organic Nano-techniques (III)*, edited by H. Morkoc (Academic Press, San Diego, CA, 2003).

[19] T. Rakshit, G.-C. Liang, A. W. Ghosh, M. C. Hersam and S. Datta, *Phys. Rev. B* **72**, 125305 (2005).

[20] F. Zahid, M. Paulsson, E. Polizzi, A. W. Ghosh, L. Sidiqui, and S. Datta, *J. Chem. Phys.* **123**, 064707 (2005).

[21] J. A. Pople and G. A. Segal, *J. Chem. Phys.* **44**, 3289 (1966).

[22] L. Olesen, M. Brandbyge, M. R. Sorensen, K. W. Jacobsen, E. Lgsgaard, I. Stensgaard and F. Besenbacher, *Phys. Rev. Lett.* **76**, 1485 (1996).

[23] J. Cerdá, A. Yoon, M. A. V. Hove, P. Sautete, M. Salmeron and G. A. Somorjai, *Phys. Rev. B* **56**, 15900 (1997).

[24] Original $\zeta=2.341$, Modified $\zeta=1.10427$.

[25] Y. Xue, S. Datta, S. Hong, R. Reifenberger, J. I. Henderson and C. P. Kubiak, *Phys. Rev. B* **59**, R7852 (1999).

[26] M. Di Ventra, S. T. Pantelides and N. D. Lang, *Phys. Rev. Lett.* **84**, 979 (2000).

[27] E. G. Emberly and G. Kirczenow, *Phys. Rev. Lett.* **87**, 269701 (2001).

[28] B. Muralidharan, A. W. Ghosh and S. Datta, *Phys. Rev. B* **73**, 155410 (2005).